Fuel 126 (2014) 177–187

Contents lists available at ScienceDirect

Fuel

journal homepage: www.elsevier.com/locate/fuel

Development of a gas phase combustion model suitable for low and high turbulence conditions

Ali Shiehnejadhesar [a,b,*], Ramin Mehrabian [a,b], Robert Scharler [a,b,c], Graham M. Goldin [d], Ingwald Obernberger [a,b,c]

[a] BIOENERGY 2020+ GmbH, Inffeldgasse 21b, 8010 Graz, Austria
[b] Institute for Process and Particle Engineering, Graz University of Technology, Inffeldgasse 21b, 8010 Graz, Austria
[c] BIOS BIOENERGIESYSTEME GmbH, Inffeldgasse 21b, 8010 Graz, Austria
[d] ANSYS, Inc., 10 Cavendish Court, Lebanon, NH 03766, USA

HIGHLIGHTS

- The limitation of the EDC combustion model in low turbulence conditions is argued.
- A hybrid combustion model applicable over the whole Reynolds range is introduced.
- The importance of molecular diffusion at low Reynolds number is shown.
- The simulation results are in good agreement with experimental data.

ARTICLE INFO

Article history:
Received 18 November 2013
Received in revised form 17 February 2014
Accepted 18 February 2014
Available online 12 March 2014

Keywords:
Combustion
Eddy Dissipation Concept
Finite rate kinetics
Differential diffusion
Hybrid model

ABSTRACT

A novel hybrid gas phase combustion model suitable for low as well as high turbulent combustion conditions is proposed. In particular, in the region above the fuel bed of small-scale biomass combustion plants, gas phase mixing is highly influenced by laminar and low turbulence zones. Here, the eddy break-up combustion models are not valid because they were originally developed for highly turbulent flows. Therefore, a CFD gas phase reaction model applicable over the whole Reynolds range from laminar to turbulent flows is developed. It is a hybrid Eddy Dissipation Concept/finite rate kinetics model which calculates the effective reaction rate from laminar finite rate kinetics and the turbulent reaction rate and weights them depending on the local turbulent Reynolds number of the flow. To validate the proposed model, comparisons are made with experimental data for a series of jet flames covering laminar, transitional, and turbulent flow conditions. The simulation results show that the prediction of flame can be improved with the proposed hybrid combustion model.

1. Introduction

The production and supply of energy is one of the greatest concerns of human society. With regard to the facts that the fossil fuel resources are depleting rapidly, the necessity to find new energy resources is indispensable. During recent decades, the share of energy production by biomass combustion plants has been growing, because biomass is a CO_2 neutral source of energy in a sustainable agriculture/forestry system [1]. CFD modelling is becoming increasingly important for the development and optimisation of biomass combustion plants. Here, gas phase combustion models play a key role concerning predictions of flow, temperature, and gaseous emissions (e.g. CO).

The eddy break-up models (EBU) are the most prevalent Reynolds Averaged Navier–Stokes (RANS) based combustion models which have been successfully applied for a variety of combustion plants [2–4]. The popularity of the EBU combustion models come from their low computational costs especially for industrial applications in the context of RANS simulations. However, the empirical constants in the EBU models are not universally valid and need to be adapted depending on the application [5,6]. The EBU model first was proposed by Spalding [7] and later modified by Magnussen and Hjertager [8]. The main assumption of the EBU model is based on infinitely fast chemistry and assumes that the reaction rate is

* Corresponding author at: Institute for Process and Particle Engineering, Graz University of Technology, Inffeldgasse 21b, 8010 Graz, Austria. Tel.: +43 316 8739230; fax: +43 316 8739202.
E-mail addresses: ali.shienejadhesar@gmail.com, ali.shiehnejad@bioenergy2020.eu (A. Shiehnejadhesar).

http://dx.doi.org/10.1016/j.fuel.2014.02.040
0016-2361/

Nomenclature

$C_{j,r}$	molar concentration of each reactant and product species j in reaction r (kg mol m^{-3})
C_γ	EDC model constant (–)
C_{D1}	EDC model constant (–)
C_{D2}	EDC model constant (–)
C_τ	EDC model constant (–)
d	jet diameter (m)
$D_{i,m}$	diffusion coefficient for species i in the mixture (m^2 s^{-1})
D_t	turbulent diffusivity (m^2 s^{-1})
$\vec{J}_i$	diffusion flux of species i (kg m^{-1} s^{-1})
$K_{f,r}$	forward rate constant for reaction r (s^{-1})
$K_{b,r}$	backward rate constant for reaction r (s^{-1})
k	turbulent kinetic energy (m^2 s^{-2})
$M_{w,i}$	molecular weight (kg kmol^{-1})
N	number of species
N_R	number of reactions
Re	Reynolds number (–)
Re$_t$	turbulent Reynolds number (–)
R_i	net rate of production of species i by chemical reaction (kg m^{-3} s^{-1})
$\overline{R}_{i,r}$	molar rate of creation/destruction of species i in reaction r (kg mol m^{-3} s^{-1})
S_{ct}	Schmidt number (–)
T	temperature (K)
T_r	time scale ratio (–)
Y_i	mass fraction of species i (–)

Greek symbols

ε	turbulent dissipation rate (m^2 s^{-3})
γ	length fraction of EDC fine scales (–)
ν	kinematic viscosity (m^2 s^{-1})
$\nu'_{i,r}$	stoichiometric coefficient for reactant i in reaction r (–)
$\nu''_{i,r}$	stoichiometric coefficient for product i in reaction r (–)
ρ	density (kg m^{-3})
τ_{EDC}	EDC time scale (s)
$\vec{v}$	velocity vector (m s^{-1})
μ_t	turbulent viscosity (kg m^{-1} s^{-1})

Subscript

b,r	backward reaction
EDC	Eddy Dissipation Concept
FRK	finite rate kinetics
f, r	forward reaction
i	species index
r	reaction
t	turbulent

controlled by turbulent mixing [8]. The Eddy Dissipation Concept (EDC) is an extended version of EBU model developed by Magnussen [9] which can incorporate detailed chemistry calculations in turbulent combustion. However, in the region above the fuel bed and in small-scale biomass combustion applications (size-range < 500 kWth), the gas phase mixing and reaction progress is highly influenced by laminar and low turbulence zones. Here, the EBU gas phase combustion models, which are originally developed for highly turbulent flows, are not valid, leading to wrong predictions of the reaction progress and wrong concentrations of gas species (CO, NO_x species, etc.).

The EDC, which enables the consideration of the complex interaction of turbulence and detailed reaction kinetics, was taken as a basis for the development of a general gas phase combustion model applicable for the entire Reynolds-number range of flows. However, gas phase combustion models like the EDC are originally developed for high-Reynolds-number conditions. The EDC is based on the turbulent energy cascade, which means that larger eddies break up into smaller eddies, and the reactions take place in the so-called fine structures, where the fluid is mixed on a micro-scale.

In biomass grate furnaces, in particular above the fuel bed, the flow is in the low Re range. Here, the flue gas varies from 0.5 to 2 (m/s). Moreover, in small-scale combustion plants (up to 100 kW), even the exit Reynolds number of the secondary air jets may be in the laminar to transition region. Therefore, the prediction of the flue gas species and temperature strongly depends on the CFD gas phase combustion model applied. In the EDC, the prediction mainly depends on the turbulent quantities k and ε, where a large error on the predictions is imposed when the flow approaches low Reynolds conditions. Here, it is important to simulate the combustion progress by the pure finite rate kinetics model.

Therefore, an advanced gas phase reaction model has to be developed which is sensitive regarding local flow conditions. The model should reliably distinguish between the mixing or kinetically dominated zones. Hence, a novel hybrid gas phase combustion model which utilizes combined finite rate kinetics and EDC combustion models is presented in this work. The hybrid model was implemented in ANSYS® FLUENT®.

The model development was done based on the simulation of measured jet flames by Barlow and Frank [10] (Sandia flame D as well as flame A with a jet Re number of 1100 and flame B with a jet Re number of 8200). Since it is well-known that k–ε models over-predict the spreading rate of round jets, the model constants were modified in order to minimize additional effects influencing gas phase combustion modelling. Furthermore, at low-turbulent combustion regimes the description of the reaction kinetics is of high relevance since it has a considerable influence on the simulation results.

During typical biomass combustion conditions with air staging the most relevant components released are H_2O, CO_2, CO, H_2, and CH_4 [11–13]. All these species are also relevant during Methane combustion [14,15]. Moreover, the combustion model developed can be applied together with any reaction mechanisms, which of course has to be validated for the target application. Currently, the Skeletal Kilpinen97 mechanism [16] which has extensively been validated for biomass combustion conditions is being applied [17] for biomass grate furnaces. Hence, the reduced DRM-22 reaction mechanism [15] was selected based on the simulation of Sandia flame D.

At low-Re conditions the influence of molecular diffusion on mixing becomes comparable to the influence of turbulent diffusion. Therefore, the diffusion of each gas species in the mixture was taken into account and compared with the conventional approach (constant value for the diffusion of the species in the mixture) for the simulation of flame A (Re = 1100) and B (Re = 8200). While the EDC together with the differential-diffusion (diff-diff) approach gave a good agreement with measurements for flame B with moderate turbulence, it failed to predict the laminar flame A. With finite rate kinetics (FRK) good results could be achieved for flame A. Since it could be shown that the EDC is not valid below turbulent Reynolds number of 64 [18], a hybrid EDC/FRK model is introduced. The model calculates the reaction rates with the FRK

and the EDC and finally an effective reaction rate is calculated with weight functions in dependence of the turbulent Reynolds number.

2. Methodology

Since the hybrid model is a combination of the FRK and the EDC model, a brief description of both models is given first. Next, the limitation of the EDC especially at low turbulent conditions is investigated. Finally, the hybrid model is introduced which combines the FRK and the EDC model with a weighting factor in dependence of the local turbulent Reynolds number of the flow.

2.1. Finite-rate kinetics

The FRK model computes the chemical source terms using Arrhenius expressions, and ignores the effects of turbulent fluctuations [19]. For a multi-component system, the species mass conservation equation is defined as follows;

$$\frac{\partial}{\partial t}(\rho Y_i) + \nabla \cdot (\rho \vec{v} Y_i) = -\nabla \cdot \vec{J_i} + R_i \tag{1}$$

where ρ is the mixture density, Y_i is the mass fraction of species i, $\vec{v}$ is the velocity vector, $\vec{J}_i$ is the diffusion flux of species i due to concentration gradients, and R_i is the net rate of production of species i by the chemical reactions. The net reaction source of chemical species i is computed as the sum of the Arrhenius reaction sources over the N_R reactions that the species participates in [19]:

$$(R_i)_{\mathrm{FRK}} = M_{w,i} \sum_{r=1}^{N_R} \overline{R}_{i,r} \tag{2}$$

where $M_{w,i}$ is the molecular weight of species i and $\overline{R}_{i,r}$ is the Arrhenius molar rate of creation/destruction of species i in reaction r.

The molar rate of creation/destruction of species i in reaction r ($\overline{R}_{i,r}$ in Eq. (2)) is determined:

$$\overline{R}_{i,r} = \left(\nu''_{i,r} - \nu'_{i,r}\right)\left[k_{f,r}\prod_{j=1}^{N}[C_{j,r}]^{\eta'_{j,r}} - k_{b,r}\prod_{j=1}^{N}[C_{j,r}]^{\nu''_{j,r}}\right] \tag{3}$$

where N is the number of chemical species in the system, $\nu'_{i,r}$ is the stoichiometric coefficient for reactant i in reaction r, $\nu''_{i,r}$ is the stoichiometric coefficient for product i in reaction r, $k_{f,r}$ is the forward rate constant for reaction r and $k_{b,r}$ is the backward rate constant for reaction r, $C_{j,r}$ is the molar concentration of species j in reaction r, and $\eta'_{j,r}$ is the rate exponent for reactant species j in reaction r.

2.2. EDC gas phase combustion model

The EDC is based on the turbulent energy cascade, which means that larger eddies break up into smaller eddies and the reactions take place in the so-called fine structures, where the fluid is mixed on a micro-scale. In the EDC the fluid is divided into the volume fraction of the fine structures $\gamma^* = \gamma^3$, where the reactions take place and the volume fraction $\gamma_0 = (1-\gamma^3)$ of the surroundings, which are considered as inert.

The length fraction γ of fine scales is modelled as:

$$\gamma = C_\gamma \left(\frac{v\varepsilon}{k^2}\right)^{0.25} \tag{4}$$

where C_γ is

$$C_\gamma = \left(\frac{3C_{D2}}{4C_{D1}^2}\right)^{0.25} = 2.1377, \quad \text{with} \quad C_{D1} = 0.134,\ C_{D2} = 0.5 \tag{5}$$

The time scale for the mass transfer from the fine structures to the surrounding fluid (and the residence time in the fine scales) is:

$$\tau_{\mathrm{EDC}} = C_\tau \left(\frac{v}{\varepsilon}\right)^{0.25} \quad \text{with} \quad C_\tau = \left(\frac{C_{D2}}{3}\right)^{1/2} = 0.4082 \tag{6}$$

Here, v is the kinematic viscosity; ε is the turbulent dissipation rate and k the turbulent kinetic energy.

The length fraction and the time scale sizes in terms of turbulent Reynolds number ($\mathrm{Re}_t = k^2/v\varepsilon$) can be written as following:

$$\gamma = C_\gamma (\mathrm{Re}_t)^{-1/4} \tag{7}$$

and

$$\tau_{\mathrm{EDC}} = C_\tau \mathrm{Re}_t^{-1/2} \frac{k}{\varepsilon} \tag{8}$$

There are two different approaches for the mean average reaction rate. The first one is γ^3/τ [9], while the expression γ^2/τ has been used in recent papers [20,21]. The later expression is derived assuming that the fine structures exchange mass mainly with fine structure regions and not with the whole surrounding flow [20]. Therefore, the source term in the species mass conservation equation (Eq. (1)) for the mean species i based on the recent formulation is modelled as [20];

$$(R_i)_{\mathrm{EDC}} = \rho \frac{\gamma^2 \chi}{\tau_{\mathrm{EDC}}}\left(Y_i^* - Y_i^0\right) \tag{9}$$

where the term χ is a parameter that expresses the probability that the conditions are suitable for reaction to occur in the fine structures. Y^0 is the surrounding mass fraction of species i and Y^* is the fine structure mass fraction of species i. Gran [20–22] proposed that by setting the value of $\chi = 1$, the amount of reaction is controlled by the chemistry. The relation between the mass-averaged state and the surrounding species mass fraction is computed as [20]:

$$\overline{Y}_i = \gamma^3 Y_i^* + (1-\gamma^3) Y_i^0 \tag{10}$$

The surrounding species mass fraction can be obtained from Eq. (10) as following:

$$Y_i^0 = \frac{\overline{Y}_i - \gamma^3 \chi Y_i^*}{(1-\gamma^3\chi)} \tag{11}$$

Now by substituting the surrounding species mass fraction (Eq. (11)) into Eq. (9), the final expression for the mean chemical reaction rate can be re-written as following:

$$(R_i)_{\mathrm{EDC}} = \frac{\rho\gamma^2}{\tau_{\mathrm{EDC}}(1-\gamma^3)}\left(Y_i^* - \overline{Y}_i\right) \tag{12}$$

The reactor condition in (Eq. (12)), is found from the mean values of mass fractions and enthalpy, assuming no pressure changes between surrounding and fine structure [23]. In the original formulation of the EDC [8,9] the fine structures are treated as well stirred reactors (WSR). This circumstance may lead to convergence problems during the iterative solution of the high non-linear algebraic equation system and causes a considerable numerical effort. It was shown [23] that a plug flow reactor (PFR) model can be implemented in the EDC instead of a WSR, which leads to a considerable simplification of the numerical solution process. An integration of the reaction rates over the residence time (or reaction time) in the fine structures via a time-stepping method can then be used for the calculation of the fine structure values. This is the current formulation of the EDC implemented in the CFD code ANSYS® FLUENT®.

2.3. EDC model sensitivity analysis

The EDC was originally developed for high Reynolds combustion flows. The main assumption of the model is that the reaction takes place in the so-called fine structures, which are in the order

of the Kolmogorov eddy scale, where the dissipation occurs. The EDC model was derived based on the cascade model for highly turbulent flows. Magnussen [8,9] presented the EDC cascade model with a characteristic frequency or strain rate, whereas the mechanical energy transfers from the mean flow to heat. In the EDC cascade model for the transport of mechanical energy and thermal energy from preceding level to the following one, a constant [24] has been introduced. However, for simplicity, the model assumed all constants at each level are the same. Besides, the numerical values for the model constants are derived based on an analogy with the k–ε turbulence model constants [24]. However, the applicability of the k–ε turbulence model in low Reynolds number flows is with uncertainties [25]. Thus, the choice of numerical values for the EDC model constants, indeed, affects the local combustion-rate predictions [24].

The main difference between two turbulent flows with different Reynolds numbers but with the same integral scale is the size of smallest eddies. A turbulent flow at a relatively low Reynolds number has a relatively "coarse" small-scale structure [26]. Hence at low Reynolds flow conditions, where large and small scales of turbulence are very close to each other, the applicability of the EDC model should be revised.

The influence of the EDC model constants has been reported in a few recent works [18,27–30]. Rehm et al. [27] reported the capability of the EDC for gasification modelling. They found that C_τ had almost no impact whereas the C_γ had a strong impact on the mean reaction rate and their results were improved by increasing of the C_γ constant. De et al. [18] performed a systematic EDC model sensitivity concerning the model constants. The outcomes of their study indicated that the EDC is not valid below the turbulent Reynolds number of 64. They simulated a jet in a hot co-flow and found too early ignition with the standard EDC model constants. They showed that the predictions could be improved if the C_τ is increased to 3 and C_γ is decreased to 1.0. Graça et al. [28] simulated a reversed flow small-scale combustor with the EDC and found a delayed ignition with the standard model constants. They demonstrated the dominating role of C_γ to improve the results in comparison with experiments. Shabanian et al. [29] confirmed the outcomes of De et al. [18] and used the modified C_τ constant proposed by [18,30] for the simulation of an ethylene jet flame in diluted and heated oxidant stream combustion conditions. They displayed that a modified EDC leads to reasonable results with relatively low computational effort.

Therefore, based on the above explanation, it is of interest to investigate the sensitivity of the predicted reaction rate to the model constants C_τ and C_γ. The model constant C_τ appears as a multiplication factor in the EDC time scale (Eq. (6)) as well as in the reaction rate term (Eq. (12)). In the EDC model, the reaction rate for the chemical species was assumed to be a linear function of the mass transfer between fine structures and surroundings [24]. However, it is clear from (Eq. (12)) that the characteristic time scale in the EDC model is larger than τ_{EDC}:

$$\frac{1}{\tau_{mix}} = \frac{\gamma^2}{(1-\gamma^3)}\frac{1}{\tau_{\mathrm{EDC}}} \tag{13}$$

Now, by definition of the time scale ratio (T_{ratio}), Eq. (13) can be rearranged as following:

$$T_{ratio} = \frac{\tau_{EDC}}{\tau_{mix}} = \frac{\gamma^2}{(1-\gamma^3)} \tag{14}$$

From a physical point of view, the mixing time scale τ_{mix} should be greater than the EDC time scale. Therefore, for consistency, T (and γ) should be lower than one:

$$T_{ratio} = \frac{\gamma^2}{(1-\gamma^3)} < 1 \Rightarrow \gamma < 0.75 \tag{15}$$

This implies that the fine scale length fraction (Eq. (4)) should be less than 0.75. Now by re-arranging Eq. (4) in terms of turbulent Reynolds number (Eq. (7)), the following expression can be obtained:

$$C_\gamma(\mathrm{Re}_t)^{-1/4} < 0.75 \rightarrow \mathrm{Re}_t > 64 \tag{16}$$

Fig. 1 shows the sensitivity of γ and the time scale ratio on the turbulent Reynolds number. It can be inferred from the figures that the model is limited to turbulent Reynolds numbers larger than 64. Besides, supposing that the maximum value for the fine scale length fraction is one (reaction takes place in the whole CFD computational cell), the model still has no value for the fine scale length fraction at turbulent Reynolds numbers lower than 20 (see Fig. 1 left).

As explained earlier, the assumptions of the EDC model at low turbulence flow are no longer valid. The model has no value for γ at turbulent Reynolds numbers lower than 64.

2.4. Hybrid gas phase combustion model

Based on the outcomes of the EDC sensitivity analysis, the necessity of a model which should be valid for all flow conditions is inevitable. The idea of such a reaction model which utilises the benefits of both the FRK and the EBU model first was proposed by Spalding [7]. The concept is to develop a hybrid reaction model to be sensitive to the local turbulent Reynolds number of flow. Therefore, a hybrid reaction model as a combination of both FRK as well as EDC models has been introduced. In the hybrid model, the mean chemical reaction (second term in the right hand side of Eq. (1)) is modelled as:

$$(R_i)_{\mathrm{Hybrid}} = \left(\frac{1}{1+\mathrm{Re}_t}\right)(R_i)_{\mathrm{FRK}} + \left(\frac{\mathrm{Re}_t}{1+\mathrm{Re}_t}\right)(R_i)_{\mathrm{EDC}} \tag{17}$$

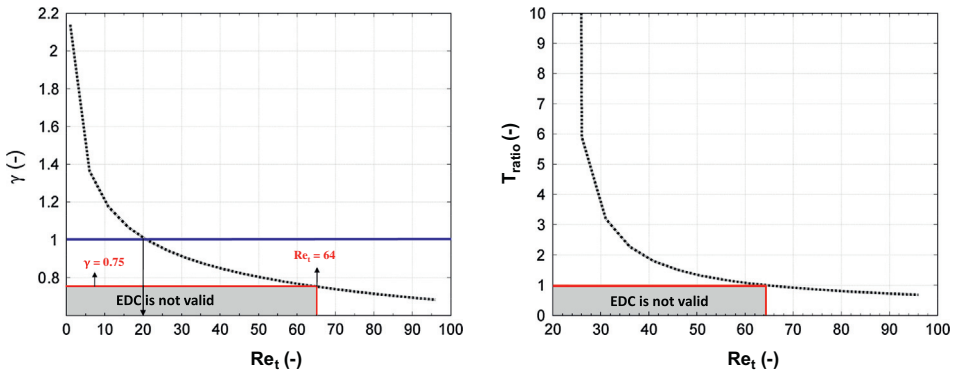

Fig. 1. Dependence of γ (Eq. (7)) (left) and T_{ratio} (Eq. (14)) (right) on turbulent Reynolds number.

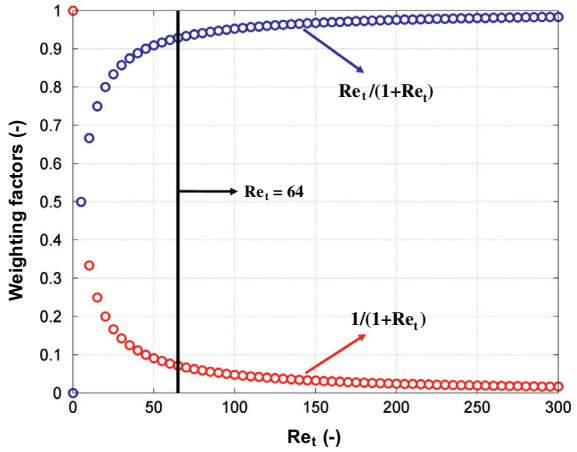

Fig. 2. Effect of turbulent Reynolds number on the weighting factors in the hybrid model.

where $(R_i)_{FRK}$ is the FRK mean reaction rate (Eq. (2)) and the term $(R_i)_{EDC}$ is the mean reaction rate calculated by the EDC model (Eq. (12)).

In the laminar range the reaction rate is calculated with pure finite rate kinetics and in the highly turbulent region with the EDC. In the transition region around $Re_t = 64$, the overall reaction rate is calculated as the sum of the weighted reaction rates of finite rate kinetics and the EDC. In other words, the overall reaction rate is determined as a linear combination of the two reaction rates.

The weighting factors $((1/1 + Re_t)$ and $(Re_t/1 + Re_t))$ are model parameters of a weight function which gave the best agreement with measurements for flames A, B and D.

The effect of weighting factors in Eq. (17) on each reaction rate as a function of turbulent Reynolds number is shown in Fig. 2.

For instance, at zero turbulence ($Re_t = 0$), the transition parameter ($Re_t/1 + Re_t = 0$) while the transition parameter ($1/1 + Re_t = 1$) and the reaction rate in controlled by the chemistry and vice versa.

3. Validation cases and numerical set-up

Three round jet flames are chosen for model validations which were measured by Barlow and Frank [10]. The flames cover laminar (flame A), transition (flame B) and turbulent (flame D) combustion conditions. The burner, consisting of a main round jet and a concentric pilot, was placed in a wind tunnel. The main jet consists of a mixture of CH_4 with air. The pilot is a lean fuel/air mixture which is active just for flames B and D for the purpose of flame stabilization, while there is no mass flow rate through the pilot for flame A. A detailed information concerning the operating conditions for flames A, B and D can be found in [10,31,32].

For all simulations, a 2D axisymmetric domain was used due to the symmetry of the burner. The computational domain extended from 10*d* behind the nozzle exit plane to 100*d* in the axial direction and 50*d* in the radial direction, where *d* is the main jet diameter. In order to estimate the velocity and turbulence quantity profiles at inlet boundaries (main jet and pilot) according to the experiments, the nozzle with a length of 10*d* was included in the computational domain. The applied CFD boundary conditions as well as the flame configuration are shown in Fig. 3.

The governing equations consist of incompressible Favre-averaged transport equations of continuity, momentum, energy, species conservation and the standard k–ε equations. The discrete ordinates (DO) radiation model [33] together with the Weighted-Sum-of-Gray-Gases (WSGG) method was used to solve the radiative heat transfer equation. A second-order upwind discretisation

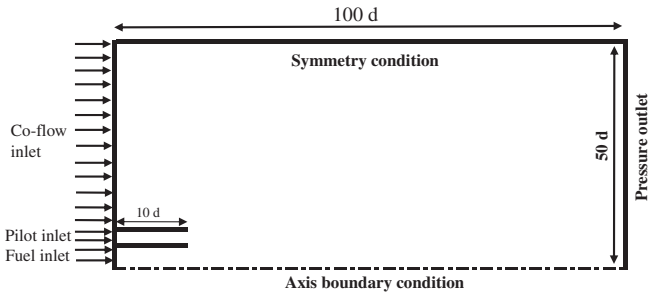

Fig. 3. Numerical model geometry and applied boundary conditions.

scheme was used to solve all governing equations. Solution convergence has been determined by two criterions. Firstly, all the residuals of the solved equations fall below the value of 10^{-6}. The second convergence criterion is to monitor the concentration of some species (e.g. CO concentration) at a specified location in the computational domain which has to be stabilised and does not change with iterations. The direct integration (DI) of the stiff ODE system of Eqs. (2) and (12) is very time-consuming due to the disparity of time-scales involved in the reaction mechanism. Therefore the In-Situ Adaptive Tabulation (ISAT) algorithm by Pope [34] has been used to speed-up the CPU-intensive treatment of the detailed reaction kinetics. In the calculations reported here the ISAT error tolerance was set to 10^{-5}.

4. Results and discussion

The simulation results for flames A, B and D are presented in this section. Firstly, flame D is used for validating the CFD grid as well as the reaction mechanism applied for the subsequent simulations. The importance of differential (molecular) diffusion at low Reynolds turbulent flames is explained later. Then, it is shown that flame A could not be simulated with the standard EDC model. The validity range of the EDC for the simulation of flames A and B is discussed and finally the simulation results with the hybrid model for all flames are shown.

4.1. Grid independence and effect of kinetic mechanisms

Two sets of structured grids of 4 and 10 k elements are studied. The grids are refined close to the nozzle and in the axial direction. A modified version of the k–ε turbulence model with the constant $C_{\varepsilon 1}$ set to 1.58 (instead of 1.44) is used for the simulation of flame D to compensate for the round jet anomaly [35–37]. However, this modification leads to an over prediction of the flame temperature in the axial direction of the flame (see Fig. 4). In this region, the temperature along the axis is determined by the mixing of the cold air with the post combustion gases. So, it strongly depends on the spreading rate determined by the turbulence model applied [38–40].

The results obtained with both grids exhibited the same performance (not shown here), therefore, the grid with 4 k cells was selected to guarantee computational accuracy and to save calculation time for subsequent simulations (flames A and B).

The influence of the reaction mechanism on the predictions for flame D is studied by using two different kinetic mechanisms. DRM-22 [15] is a reduced version of the GRI1.2. [41]. It consists of 24 species and 104 reversible reactions. The GRI2.11 [14] is a full kinetic mechanism, which consists of 49 species and 277 reversible reactions.

Fig. 4 exhibits the results obtained for flame D with both reaction mechanisms. The results are obtained with the EDC on the

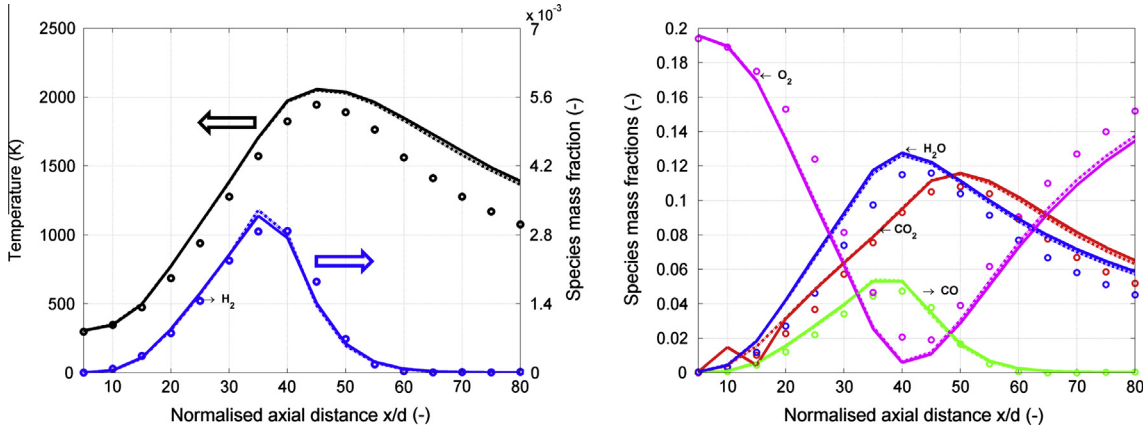

Fig. 4. Effect of chemical mechanism on the accuracy of prediction for flame D. Circles: experiment, solid lines: GRI 2.11 mechanism, dashed dotted lines: DRM-22 mechanism.

benchmark CFD grid (4*k* cells) with a modified k–ε turbulence model. The results show that the performance of the DRM-22 mechanism is identical to the detailed GRI2.11 mechanism. Hence, the DRM-22 is used for the further simulations.

Table 1
Modified $C_{\varepsilon 1}$ values used in the simulations for flames A and B.

Flame	A	B
$C_{\varepsilon 1}$	11	4

4.2. 2Molecular diffusion effect

In turbulent flows the turbulent diffusion generally overwhelms laminar diffusion, and the specification of detailed laminar diffusion properties in turbulent flows is usually not necessary. The diffusion flux (J_i) in Eq. (1) is defined as

$$J_i = -\left(\rho D_{i,m} + \frac{\mu_t}{Sc_t}\right)\nabla Y_i \tag{18}$$

where the first term on the right-hand side of Eq. (18) is molecular diffusion and the second term expresses the turbulent diffusion. The term, $D_{i,m}$ is the mass diffusion coefficient for species i in the mixture, and $Sc_t = \mu_t/\rho D_t$ is the turbulent Schmidt number (where μ_t is the turbulent viscosity and D_t is the turbulent diffusivity). However, under combustion conditions at low Reynolds numbers the effect of molecular diffusion on mixing becomes comparable to the turbulent diffusion at certain regions in the flame. This is mainly due to the laminarisation of the flow caused by high temperatures in the reaction zones [42]. The effect of molecular diffusion becomes more important when there is H_2 in the fuel jet stream and the jet Reynolds number is lower than 10,000 [43]. In order to highlight the effect of differential diffusion (diff-diff) on the accuracy of the predictions, the simulation of flame B (using EDC with DRM-22 mechanism) is performed with and without the effect of molecular diffusion. To account for the effect of differential diffusion in the simulation, diffusion coefficients for each species were represented as a fourth-order polynomial function of temperature. Fig. 5 shows the temperature and species mass fraction profiles which have been compared with experimental data at $x/d = 30$. The mean mixture fraction is computed using Bilger's formula [44]. The results show the significant role of differential diffusion in the accuracy of predictions. It is evident that the flame temperature is underestimated considerably (25%) in case of complete exclusion of molecular diffusion in the simulation. The minor species (H_2 and OH) mass fraction predictions are remarkably improved by more than 80% when the molecular diffusion is considered in the simulation. Ignoring differential diffusion has also caused peak H_2O and CO values being under-predicted by 20% and 60%, respectively. As a result, the effect of differential diffusion at combustion of low and moderate Reynolds numbers cannot be disregarded.

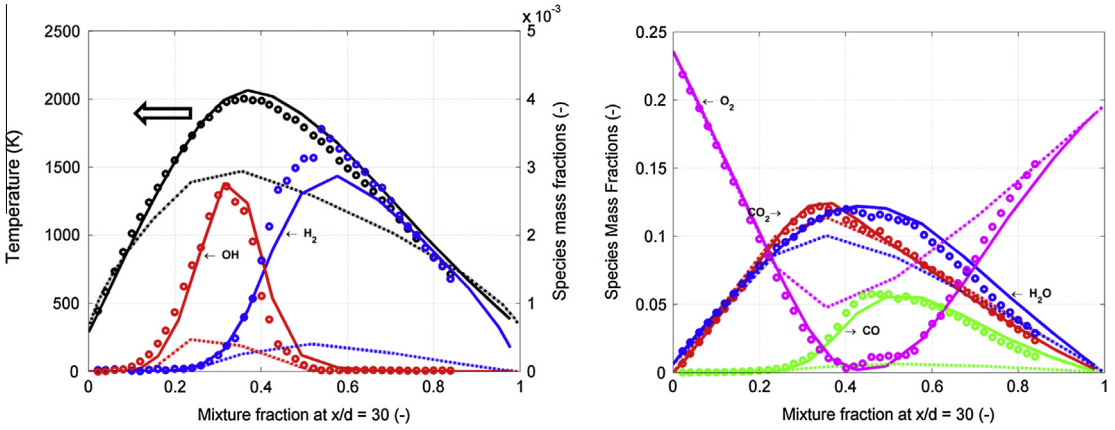

Fig. 5. Effect of differential diffusion (diff-diff) on the prediction of temperature and species mass fractions for flame B at $x/d = 30$ (–) (EDC with modified k–ε turbulence model and DRM-22 mechanism). Circles: experiment, solid lines: diff-diff effect included, dashed dotted lines: diff-diff effect excluded in the simulation.

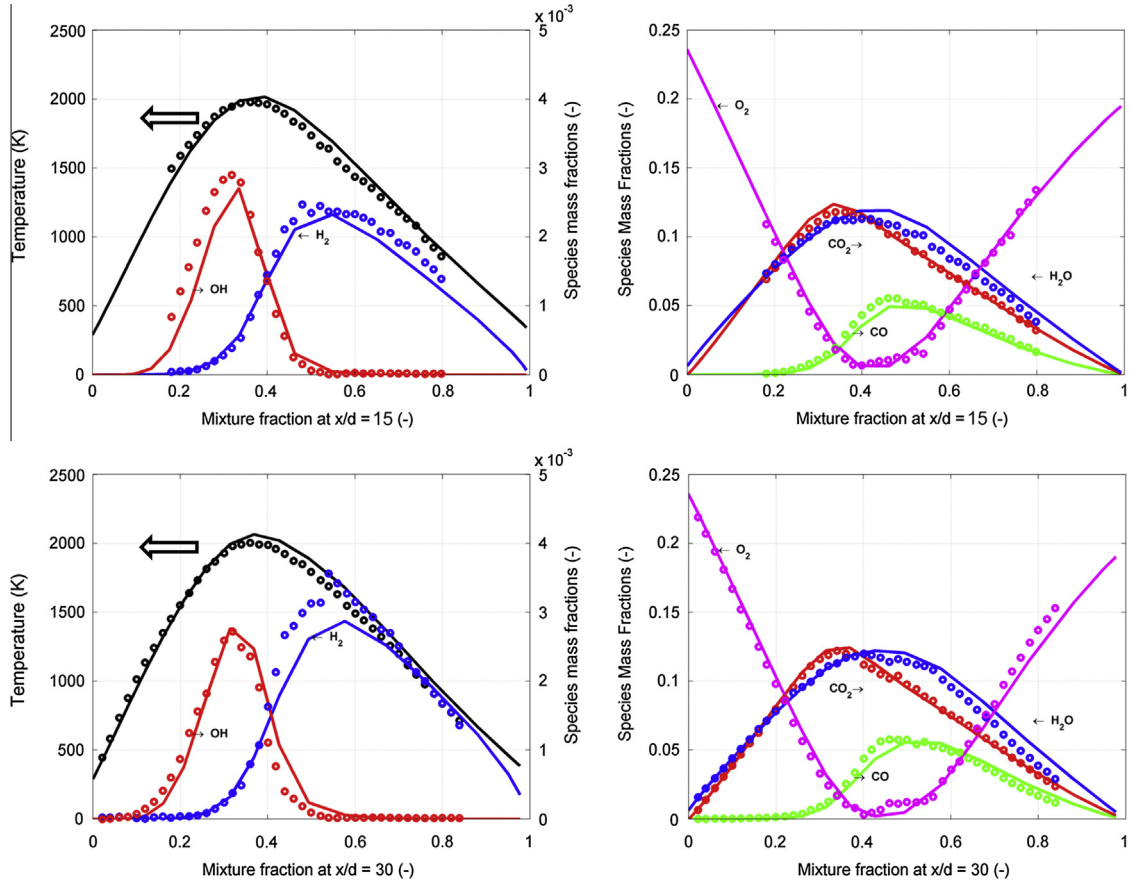

Fig. 6. Radial profiles of temperature and species mass fractions at different normalised heights of flame B (the EDC model with modified k–ε turbulence model and DRM-22 mechanism, diff-diff effect included).

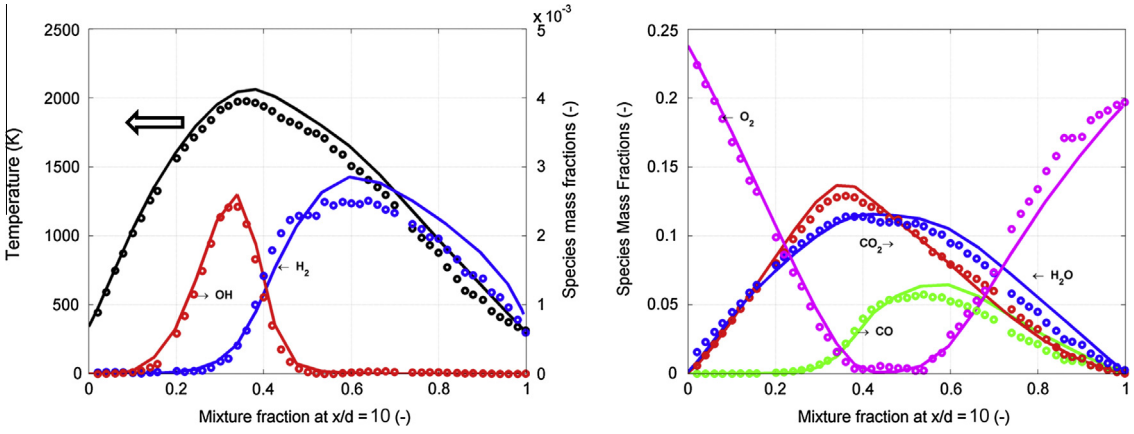

Fig. 7. Radial profiles of temperature and species mass fractions for flame A at x/d = 10 (–) (FRK model with modified k–ε turbulence model and DRM-22 mechanism, diff-diff effect included).

4.3. 3Evaluation of the standard EDC at low Reynolds conditions

For the evaluation of the standard EDC at low and moderate Reynolds number, the simulation results for flames A (laminar) and B (transitional) are presented. Flame A was mainly chosen for the evaluation of the standard EDC due to its similar flow conditions prevailing above the fuel bed in biomass combustion plants. As explained, in the region above the fuel bed the gas phase mixing and reaction progress is highly influenced by laminar and low turbulent zones. As shown in Section 2.3, the standard EDC model is not valid in regions with turbulent Reynolds number less than 64. Therefore, the standard EDC model can be tested for model evaluation at a low turbulent regime in case of flame A.

It is worth mentioning, that the experimental data were available at only two different positions (x/d = 15 and x/d = 30) for flame B and at one position for flame A (x/d = 10) including the temperature and species mass fraction profiles [10]. The standard k–ε turbulence model with a modified $C_{\varepsilon 1}$ constant is used in the simulations. The modified constants are given in Table 1.

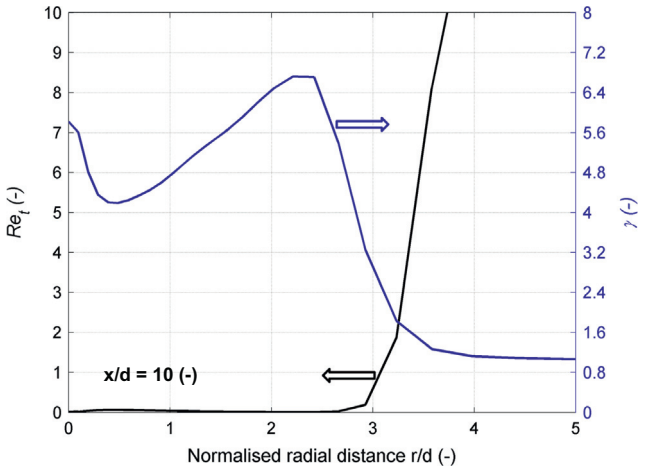

Fig. 8. Radial profiles of Re_t (left vertical axis) and, γ (Eq. (7)) (right vertical axis) for flame A at $x/d = 10$ (–) (FRK model with modified k–ε turbulence model and DRM-22 mechanism, diff-diff effect included).

Fig. 6 shows the simulation results for flame B in comparison with measurement data at $x/d = 15$ and $x/d = 30$, respectively. The results are in good agreements with measurement data at both heights. The results show that the standard EDC together with the differential diffusion approach gave satisfactorily results in comparison with experimental data even in moderate Reynolds number conditions.

For the simulation of flame A, the flame was piloted artificially by means of a small fluid zone attached to the nozzle outlet with a fixed high temperature value. This zone acted as an ignitor to establish the flame. However, flame A could not be simulated with the standard EDC even with artificial piloting. Fig. 7 demonstrates the simulation results obtained with the FRK model against experimental data for flame A. The results are in good agreement with experimental data even for minor species (H_2 and OH) profiles. This clearly indicates a good performance of the DRM-22 mechanism and the diffusion model used in this study. However, the flame temperature as well as species mass fraction profiles are somewhat over-predicted on the fuel lean side of the flame. The diffusion model plays, indeed, an important role to predict the flame characteristics properly.

The EDC sensitivity analysis presented in Section 2.3 confirmed that the model is not valid below the turbulent Reynolds number of 64. Therefore, flames A and B are chosen to analyse the validity range of the model. Fig. 8 shows the distribution of the turbulent Reynolds number (Re_t) and the fine scale length fraction γ (Eq. (4)) in radial direction at $x/d = 10$ for flame A. Since flame A could not be simulated with EDC, the fine scale length fraction was calculated according to Eq. (4) from the turbulent quantities k and ε (simulation with the FRK model together with the modified k–ε turbulence model). It is obvious that for flame A Re_t is lower than 64 in the whole reaction zone, therefore, the EDC is not valid.

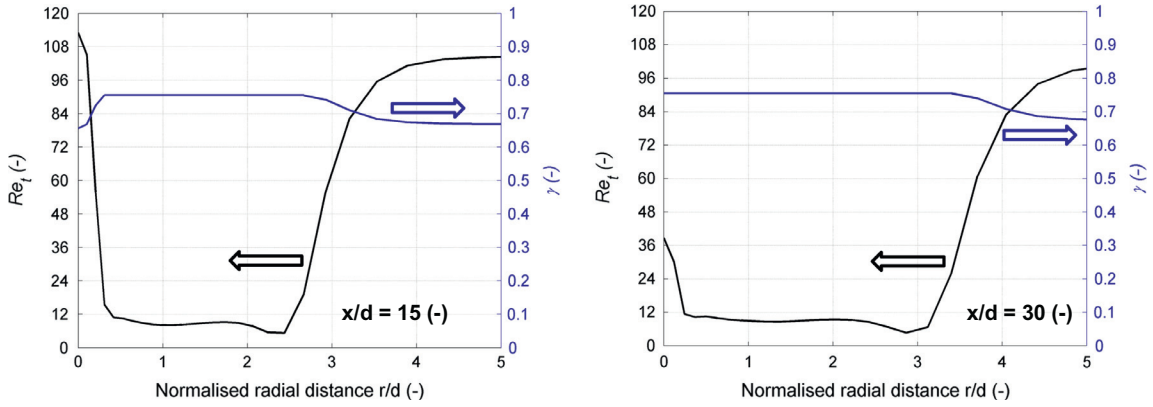

Fig. 9. Radial profiles of Re_t (left vertical axis) and, γ (Eq. (7)) (right vertical axis) for flames B (EDC with modified k–ε turbulence model and DRM-22 mechanism, diff-diff effect included).

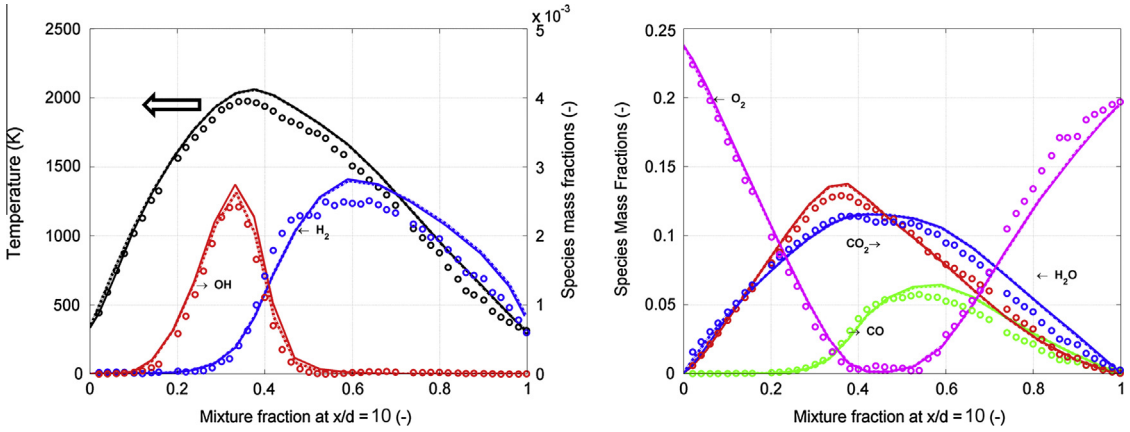

Fig. 10. Radial profiles of temperature and species mass fractions for flame A at $x/d = 10$ (–) calculated with FRK and the hybrid model (modified k–ε turbulence model, DRM-22 mechanism and diff-diff effect included). Circles: experiment, solid lines: FRK model, dashed dotted lines: hybrid model.

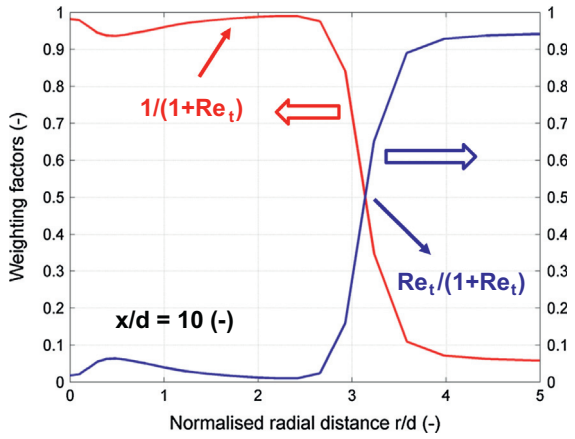

Fig. 11. Effect of weighting factors on the reaction rate calculation for flame A at $x/d = 10$ (–).

The distribution of both turbulent Reynolds number (Re_t) and the fine scale length fraction at two different heights are also presented in Fig. 9 for flame B. The turbulent Reynolds number even for flame B is generally low. Furthermore, it could be shown that the implemented EDC model in ANSYS® FLUENT® truncates the fine scale length fraction value to 0.75 for any value of Re_t lower than 64, in order to avoid non-physical values of this quantity.

It can be concluded that the standard EDC model performs well even in moderate turbulence regimes. However, the results for flame B showed that the unphysical behaviour of the mean reaction rate is prevented by clipping the fine scale length fraction to 0.75. This behaviour of the EDC model is also reported in [18], whereas the jet Reynolds number is lower than 5000.

In case of flame A, the EDC model even cannot simulate the flame since the whole reaction domain is out of the EDC validity range.

4.4. Test of the hybrid combustion model

Fig. 10 shows the predicted temperature and species mass fraction profiles for flame A with the hybrid model in comparison with the pure FRK model as well as experimental data. The results obtained with the hybrid model are similar to the pure FRK model. This implies that at low Reynolds conditions the model performs approximately as the FRK model.

The effect of weighting factors on the reaction rate calculations is also shown in Fig. 11 at $x/d = 10$ for flame A. The figure shows that the term $(1/(1 + Re_t))$ in the reaction zone takes the value of unity, therefore, the reaction rate is calculated based on the FRK part in the hybrid model.

The results predicted with the hybrid model for flame B at two different heights are shown in Fig. 12. The results were also compared with the standard EDC and the FRK models. The predictions with the hybrid model show better performance than the EDC model due to the sensitivity of the model to the locally too low turbulent Reynolds number of the flow.

The characteristics of reacting radicals are of high relevance for an in-depth understanding of the formation process of combustion emissions. Therefore, both reaction mechanism and gas phase

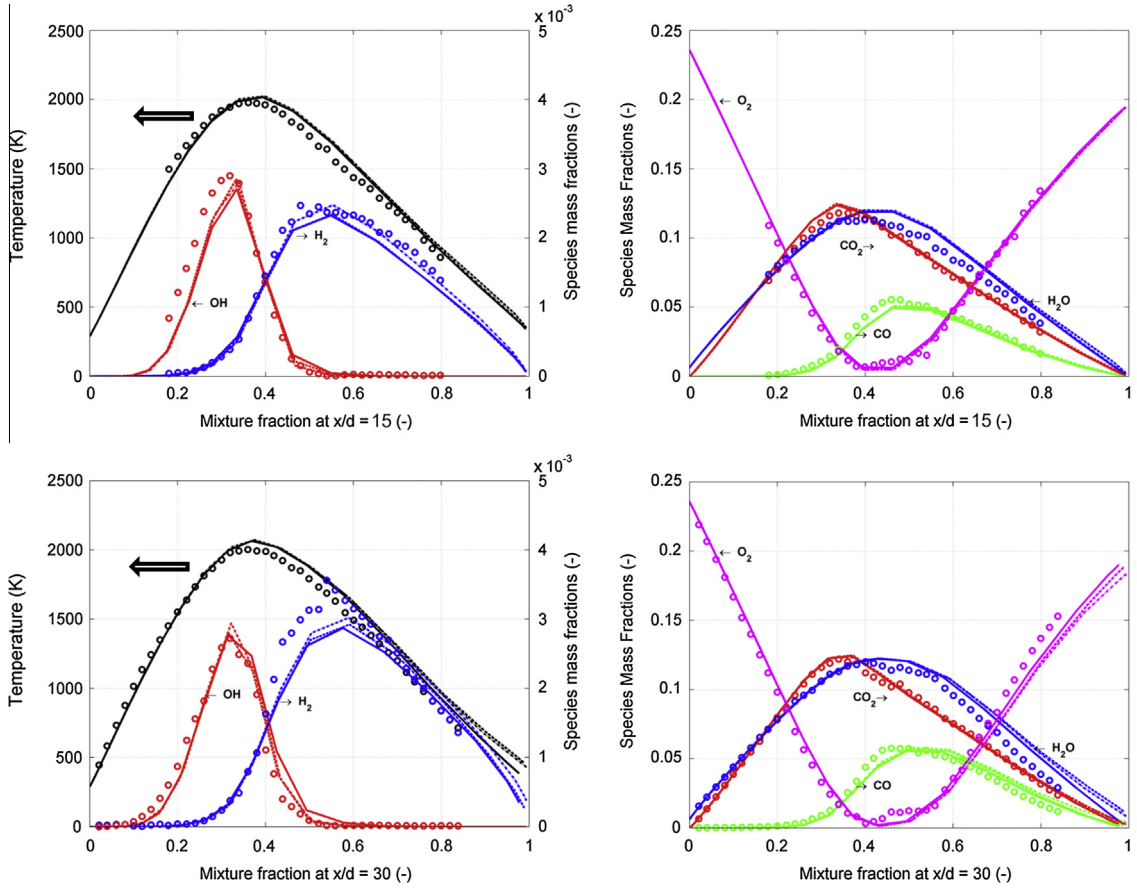

Fig. 12. Radial profiles of temperature and species mass fractions for flame B at different heights calculated with EDC, FRK and the hybrid model (modified k–ε turbulence model, DRM-22 mechanism and diff-diff effect included). Circles: experiment, solid lines: EDC model, dashed lines: FRK and dashed dotted lines: hybrid model.

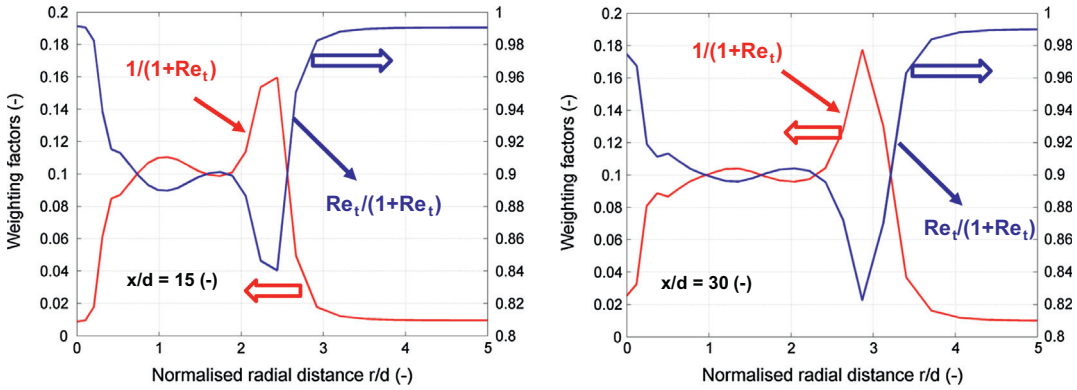

Fig. 13. Effect of weighting factors on the reaction rate calculation for flame B at different heights.

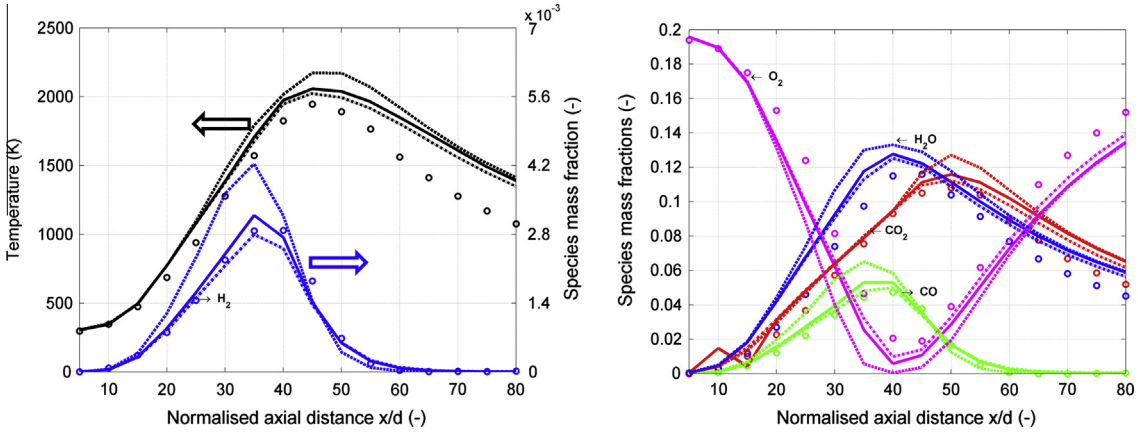

Fig. 14. Temperature and species mass fractions predictions for flame D at different normalised axial distances calculated with EDC, FRK and hybrid model (modified k–ε turbulence model, DRM-22 mechanism). Circles: experiment, solid lines: EDC model, dashed lines: FRK model and dashed dotted lines: hybrid model.

reaction model play an important role for the better prediction of radicals in the combustion simulation.

The results show that both H_2 and OH mass fraction profiles at both heights are slightly improved with the hybrid model. This is mainly because of the lower turbulent Reynolds number than the critical value (see Fig. 9) at these heights, therefore, the contribution of the FRK part in the hybrid model becomes more relevant. The effect of weighting factors on the reaction rate calculation is also presented in Fig. 13 for flame B at two different heights. The figure shows that the FRK weighting term ($1/(1 + Re_t)$) has a small effect (maximum value of 0.12 at the height of $x/d = 15$ and 0.18 at the height of $x/d = 30$) on the overall reaction rate calculation at both heights.

Fig. 14 shows the evaluation of the hybrid model for flame D in comparison to the standard EDC as well as the FRK model along the normalised axial direction of the flame. The results show that the temperature and species mass fractions are over-predicted with the pure FRK model. The obtained results with the EDC model indicate that by considering the effect of turbulence in the reaction rate calculation, the over-prediction of temperature and consequently the species mass fractions caused by the FRK model are supressed. Although the turbulent Reynolds number is by far higher than $Re_t = 64$, the FRK part in the hybrid model has a small contribution to the reaction rate calculation. The results obtained with the hybrid model show a slight improvement on the predictions. This is mainly due to a contribution of the FRK part in the overall reaction rate calculation, where the predicted CO and O_2 species are improved, respectively. The same behaviour is true also for the predicted CO_2 and H_2O species calculated with the hybrid model.

5. Summary and conclusion

A new hybrid gas phase combustion model suitable from laminar to turbulent combustion flows is presented. The hybrid model is a combination of FRK and EDC models, where the reaction rate is weighted by the local turbulent Reynolds number of the flow. The lower the turbulent Reynolds number of the flow, the greater the contribution of the FRK model to the overall reaction rate calculation in the hybrid model and vice versa. The hybrid model was programmed in C and coupled with ANSYS® FLUENT®. Also, the limitation of the EDC at low Reynolds turbulent combustion was shown. The EDC sensitivity analysis regarding model constants showed that the EDC is not valid for turbulent Reynolds numbers lower than 64. Furthermore, the CFD results obtained for flames A (Re = 1100) and B (Re = 8200) confirmed that the differential diffusion has a profound effect on the accuracy of predictions at low Reynolds combustion flows. It was found that the standard EDC was not able to establish flame A, where most of the reaction zones are located outside of the validity range of the EDC model. The results with the hybrid model for all flames showed good agreements with measurement data. The results obtained with hybrid and FRK models for flame A outline that the hybrid model performs very similarly to the pure FRK model, since the reaction zones for this flame are out of the EDC validity range.

The simulation results for flame B with the standard EDC model show good agreements with experimental results. However, the simulation with the hybrid model exhibited better performance to predict the radicals (e.g. OH and H_2). The better performance of the hybrid model in case of flame B can be explained by a greater

contribution of the FRK model to the overall reaction rate calculation. Moreover, the simulated results with the hybrid model for flame D show a better performance of the hybrid model in comparison to the EDC and the pure FRK models.

Concluding, the hybrid model displayed a great potential for application in all ranges of flow conditions and can be applied for an improved prediction of gas phase combustion in biomass combustion plants. The model can also be applied for an improved NO_x prediction since it captures radicals with better accuracy than the standard EDC model.

Acknowledgement

The author wishes to thank Dr. Barlow at Sandia National Laboratories for providing the data for flames A and B on request and helpful comments on the manuscript.

References

[1] Mehrabian R, Zahirovic S, Scharler R, Obernberger I, Kleditzsch S, et al. A CFD model for thermal conversion of thermally thick biomass particles. Fuel Process Technol 2012;95:96–108.
[2] Mancini M, Weber R, Bollettini U. Predicting NO_x emissions of a burner operated in flameless oxidation mode. Proc Combust Inst 2002;29(1):1115–63.
[3] Peters AAF, Weber R. Mathematical modeling of a 2.25 MWt swirling natural gas flame. Part 1: Eddy break-up concept for turbulent combustion; probability density function approach for nitric oxide formation. Combust Sci Technol 1995;110–111:67–101.
[4] Xue H, Ho JC, Cheng YM. Comparison of different combustion models in enclosure fire simulation. Fire Saf J 2001;36(1):37–54.
[5] Scharler R, Fleckl T, Obernberger I. Modification of a Magnussen constant of eddy dissipation model for biomass grate furnaces by means of hot gas in-situ FT-IR absorption spectroscopy. Prog Comput Fluid Dyn Int J 2003;3:102–11.
[6] Yaxin S, Cuiwu C, Along S. Simulation of high temperature air combustion with modified eddy-break-up combustion model. Energy Proc 2012;14:127–32. http://dx.doi.org/10.1016/j.egypro.2011.12.90.
[7] Spalding DB. Mixing and chemical reaction in steady confined turbulent flames. Symp (Int) Combust 1971;13:649–57.
[8] Magnussen BF, Hjertager BH. On mathematical modeling of turbulent combustion with special emphasis on soot formation and combustion. Proc Combust Inst 1977;16(1):719–29. http://dx.doi.org/10.1016/S0082-0784(77)80366-4.
[9] Magnussen BF. On the structure of turbulence and a generalized eddy dissipation concept for chemical reaction in turbulent flow. In: 19th AIAA aerospace science meeting, St. Louis, Missouri, USA; 1981.
[10] Barlow RS, Frank JH. Effects of turbulence on species mass fractions in methane/air jet flames. Proc Combust Inst 1998;27:1087–95.
[11] Neves D, Thunman H, Matos A, Tarelho L, Gomez-Barea A. Characterization and prediction of biomass pyrolysis products. Prog Energy Combust 2011;37:611–30.
[12] Boroson ML, Howard JB, Longwell JP, Peters WA. Product yields and kinetics from the vapor phase cracking of wood pyrolysis tars. AIChE J 1989;35:120–8.
[13] Graham RG, Bergougnou MA, Overend RP. Fast pyrolysis of biomass. J Anal Appl Pyrol 1984;6:95–135.
[14] Bowman CT, Hanson RK, Davidson DF, Gardiner WC, Lissianski V, Smith GP, et al. <http://www.me.berkeley.edu/gri_mech/>.
[15] Kazakov A, Frenklach M. <http://www.me.berkeley.edu/drm/>.
[16] Kilpinen P. pia.kilpinen@uku.fi or pia.kilpinen@abo.fi.
[17] Zahirovic S, Scharler R, Kilpinen P, Obernberger I. A kinetic study on the potential of a hybrid reaction mechanism for prediction of NOx formation in biomass grate furnaces. Combust Theor Model 2011;15:645–70.
[18] De A, Oldenhof E, Sathiah P, Roekaerts DJEM. Numerical simulation of delft-jet in-hot-coflow (DJHC) flames using the eddy dissipation concept model for turbulence-chemistry interaction. Flow Turbul Combust 2011;87:537–67.
[19] ANSYS® Academic Research. Release 14.0. Help System, FLUENT User Guide, ANSYS Inc.
[20] Gran IR, Magnussen BF. Numerical study of a bluff-body stabilized diffusion flame, Part 2. Influence of combustion modeling and finite-rate chemistry. Combust Sci Technol 1996;119:191–217.
[21] Magel HC, Schnell U, Hein KRG. Simulation of detailed chemistry in a turbulent combustor flow. Symp (Int) Combust 1996;26(1):67–74. http://dx.doi.org/10.1016/S0082-0784(96)80201-3.
[22] Gran IR. Mathematical modeling and numerical simulation of chemical kinetics in turbulent combustion. Ph.D. thesis, Dept. of Applied Mechanics, Thermodynamics and fluid dynamics, Norwegian University of Science and Technology, Trondheim, Norway; 1994.
[23] Jessee JP, Gansman RF, Fiveland WA. Calculation of chemically reacting flows using finite rate kinetics. Heat Transfer in Fire and Combustion System (ASME ed.) 1993;250:43–53.
[24] Eetesvåg IS, Magnussen BF. The eddy dissipation turbulence energy cascade model. Combust Sci Technol 2000;159(1):213–35.
[25] Perot JB, Bruyn Kops S de. Modeling turbulent dissipation at low and moderate Reynolds numbers. J Turbul 2006;7(69):1–14.
[26] Tennekes H, Lumley JL. A first course in turbulence. USA: MIT Press; 1972. p. 21–2.
[27] Rehm M, Seifert P, Meyer B. Theoretical and numerical investigation on the EDC model for turbulence-chemistry interaction at gasification conditions. Comput Chem Eng 2009;33:402–7.
[28] Graça M, Duarte A, Coelho PJ, Costa M. Numerical simulation of a reversed flow small-scale combustor. Fuel Process Technol 2012;107:126–37.
[29] Shabanian SR, Medwell PR, Rahimi M, Frassoldati A, Cuoci A. Kinetic and fluid dynamic modeling of ethylene jet flames in diluted and heated oxidant stream combustion conditions. Appl Therm Eng 2013;52:538–54.
[30] Aminian J, Galletti C, Shahhosseini S, Tognotti L. Numerical investigation of a MILD combustion burner: analysis of mixing field, chemical kinetics and turbulence-chemistry interaction. Flow Turbul Combust 2012;88:597–623.
[31] Schneider Ch, Dreizler A, Janicka J. Flow field measurements of stable and locally extinguishing hydrocarbon-fuelled jet flames. Combust Flame 2003;135(1–2):185–90.
[32] Barlow RS, Frank JH. SandiaPilotDoc21.pdf. <http://www.sandia.gov/TNF/DataArch/FlameD.html>.
[33] Smith TF, Shen ZF, Friedman JN. Evaluation of coefficients for the weighted sum of gray gases model. J Heat Transf 1982;104:602–8.
[34] Pope SB. Computationally efficient implementation of combustion chemistry using in situ adaptive tabulation. Combust Theor Model 1997;1:41–63.
[35] Morse AP. Axisymmetric turbulent shear flows with and without swirl. Ph.D. thesis. England: London University; 1977.
[36] Pope SB. An explanation of the turbulent round-jet/plane-jet anomaly. AIAA J 1978;16(3):279–81.
[37] Aminian J, Galletti C, Shahhosseini S, Tognotti L. Key modeling issues in prediction of minor species in diluted-preheated combustion conditions. Appl Therm Eng 2011;31:3287–300.
[38] Merci B et al. Application of a new cubic turbulence model to piloted and bluff-body diffusion flames. Combust Flame 2001;126:1533–56.
[39] Merci B, Dick E. Influence of computational aspects on simulations of a turbulent jet diffusion flame. Int J Numer Method H 2003;13(7):887–98.
[40] Zahirovic S, Scharler R, Kilpinen P, Obernberger I. Validation of flow simulation and gas combustion sub-models for the CFD-based prediction of NOx formation in biomass grate furnaces. Combust Theor Model 2010;15(1):61–87.
[41] Frenklach M, Wang H, Yu CL, Goldenberg M, Bowman CT, Hanson RK, et al. <http://www.me.berkeley.edu/gri_mech/>.
[42] Christo FC, Dally BB. Modeling turbulent reacting jets issuing into a hot and diluted coflow. Combust Flame 2005;142:117–29.
[43] Barlow RS, Frank JH, Karpetis AN, Chen JY. Piloted methane/air jet flames: transport effects and aspects of scalar structure. Combust Flame 2005;143:433–49.
[44] Bilger RW, Starner SH, Kee RJ. On reduced mechanisms for methane/air combustion in nonpremixed flames. Combust Flame 1990;80:135–49.